PCCP

Accepted Manuscript

ROYAL SOCIETY OF CHEMISTRY

www.rsc.org/pccp

Modulating Triphenylamine-based Organic Dyes for Their Potential Application in Dye-Sensitized Solar Cell: A First Principle Theoretical Study

Narendranath Ghosh,[†] Arnab Chakraborty,[†] Sougata Pal,[*,†] Anup Pramanik,[‡] and Pranab Sarkar[‡]

Department of Chemistry, University of Gour Banga, Malda- 73 2103*, India, and Department of Chemistry, Visva-Bharati University, Santiniketan-* 731 235*, India*

E-mail: sougatapal_1979@yahoo.co.in

Abstract

By using computational methodologies based on time dependent density functional theory (TDDFT) we study opto-electronic properties of three types of triphenylamine (TPA)-based dyes, naming TPA-TBT-1, TPA-DBT-1, and TPA-BT-1, and these are proposed as potential candidates for photovoltaic applications. Energy band modulation has been performed by functionalizing these dyes with different electron donating and electron withdrawing groups. Photoelectron spectra and photovoltaic properties of the dyes have been investigated by the combination of (DFT), and (TDDFT) approaches. Based on the optimized molecular geometry, relative position of the frontier energy levels, and the absorption maximum of the dyes we propose some dyes offering good photovoltaic performance. At the same time, these results provide a direction for optimizing composition of dye-metal surface nanodevice for fabricating dye-sensitized solar cell (DSSC).

[*]To whom correspondence should be addressed
[†]University of Gour Banga
[‡]Visva-Bharati University

INTRODUCTION

Dye-sensitized solar cells (DSSCs) have attracted considerable attention in recent years as they offer the possibility of low-cost conversion from photon to electrical energy and thus they have been regarded as the next generation photovoltaics.[1,2] Although ruthenium-based sensitizer[3,4] offers an overall light-to-electricity energy conversion efficiency over 11%, the limited resources and the environmental issues relating to ruthenium use make it necessary to look after alternative dyes. In this regard organic dyes have received much attention due to their environment friendly nature, low cost for device fabrication and easy preparation process.[5–9] Another major advantages of these metal-free dyes are their tunable absorption and electrochemical properties through suitable molecular design.[10]

Among the different DSSC, the bulkheterojunction model (BHJ)[11–13] is the most successful one. A DSSC is composed of four elements, namely, transparent conducting and counter conducting electrodes, wide band-gap semiconductor surface (such as TiO_2, ZnO etc.), a dye molecule (sensitizer), and an electrolyte [commonly a redox couple, I_3^-/I^- (μ=4.80 eV)].[14] The working principle of DSSC involves photoexcitation of dye molecule thereby generation of electron-hole pair. In the subsequent step, the photo excited electron is injected to the semiconductor surface followed by its diffusion to the transparent electrode. The cycle is completed via the regeneration of electron into the dye through counter electrode and electrolyte. In this regard TiO_2 is the mostly used semiconducting surface the conductance band of which is located at 4.0 eV.[15–17] From the static energetic point of view, the most crucial steps of a photovoltaic cell are the injection and regeneration process as stated above. To facilitate these two processes the following criteria should be met. (1) The lowest unoccupied molecular orbital (LUMO) energy level of the dye molecule must lie above conduction band of the semiconductor (E_{CB}) at least by 0.2-0.3 eV. (2) The highest occupied molecular orbital (HOMO) of the dye must be at lower energy than the chemical potential of the redox couple (μ_{redox}).[18,19] During this whole electronic dynamic process, the electron injection efficiency to the CB of the semiconductor surface and the electron collection efficiency at the transparent conductive electrode directly determine the short circuit current density (J_{SC}) of

DSSC. The potential difference between the Fermi level of electrons in the semiconductor substrate and the redox potential of the electrolyte gives the open circuit photovoltage (V_{OC}). These two parameters are important factors determining the energy conversion efficiency of DSSC,

$$\eta = \frac{FF * J_{SC} * V_{OC}}{P_{inc}} \quad (1)$$

where, FF is the fill factor at which DSSC operates with the maximum power, which is mainly related to the total series resistance of the DSSC. P_{inc} is the input power of incident solar light. However, it should be pointed out the overall efficiency of DSSC also depends on some other parameters like recombination series resistance, etc. Obviously, an embedded dye over a particular metal oxide plays a key role in the energy conversion efficiency of a DSSC. Generally, metal-free organic sensitizers are constituted by donor (D), π-bridge (π), and acceptor (A) moieties, so called D-π-A character. This push-pull structure can induce the intramolecular charge transfer (ICT) from subunit A to D through the π-bridge when the dye is irradiated to sunlight. This is important for harvesting solar energy. In order to act as an efficient dye in the BHJ cell, it must have the following characteristics: i) the dye must show broad absorption spectra covering whole UV and visible region to absorb maximum energy coming from light, ii) it should have low band gap, iii) it should be able to prevent electron-hole recombination effectively, iv) the dye should show high oscillator strength, v) open circuit voltage of the dye must be very high, vi) HOMO of the dye must lie below the HOMO of the redox couple and LUMO of the dye must lie above the LUMO of the conduction band (CB) of the semiconductor for swift downhill movement of electron and uphill movement of hole, and vii) a good anchoring group must be added to the dye to anchor well on the semiconductor surface.[2] As the electronic energy levels of an organic dyes are tunable by varying donor-acceptor moieties, it is possible to design an dye with desired energy levels. An enormous effort is being given in this purpose during the last couple of years.[12,20,21] One of the most interesting topics in the field of organic photovoltaics in past twenty years is to design, synthesis of low band-gap organic conducting materials for the use in the DSSCs.[22]

Polyheterocyclic molecules have attracted much attention for application in DSSCs due to

their electronic and photonic properties.[23,24] Triphenylamine (TPA) is one such kind of molecule, the excellent electron donating power and its huge steric hindrance give it the ability to prevent undesired dye aggregation at semiconductor surface.[25,26] The dyes composed of TPA as donor and cyanoacetic acid as acceptor/linker are of mammoth interest in recent time.[26,27] Yanagida and co-workers first used the TPA unit as an electron donor in organic dyes and obtained a high photocurrent efficiency (5.3%) for the dye $(Ph)_2$N-Ph-CH=CH-CH=CH(CN)COOH.[10] Compounds like (2Z)-2-cyano-3-[4-(diphenylamino) phenyl] acrylic acid and (2Z)-2-cyano-3-4-[[4-(diphenylamino)-phenyl](phenyl) amino] phenylacrylic acid has been synthesized successfully and the overall conversion efficiency of the dyes are 2.51% and 4.12%, respectively.[28] A highly advantageous thing about TPA is that, enormous range of substitutions can be done to it to meet the conditions for an efficient donor. Exploring this quality verity of p-substituted TPA derivatives have been created and they are found to perform as excellent donors.[29,30] A compound with TPA as donor and rhodanine-3-acetic acid linked by -C=C π-spacer shows photocurrent efficiency (PCE) of 4.3% but upon suitable substitution PCE reaches up to 6.3%.[25]

In general, electron deficient units are found to perform well as acceptor. For a fixed donor moiety, the acceptors like 1,2,3-benzothiadiazole (BT), thiadiazolo[3,4-c]pyridine (PyT) are found to decrease the LUMO level of the composite system without altering the HOMO level and thus low band gap material is obtained.[31–36] Thus these can be considered as good acceptors. In the development of TPA based dyes, it has been found that the above combination gives the greater efficiency in every case compared to other accepting/anchoring groups.[2]

The TPA unit is very well-known for its strong electron-donating ability and hole-transport properties. Large number of TPA based dyes show good power conversion efficiency in DSCs.[37–40] Very recently, a series of triphenylamine-based dyes with multiple corhodanine derivatives as acceptors are synthesized and reported as sensitizers for dye-sensitized solar cells with a maximum PCE of 5.31%.[41] Nevertheless, the scope is always open to further design and develop more efficient TPA dyes. In this paper we take an opportunity to perform computational studies on some newly designed TPA-base dyes with D-π-A architecture. Further modifications have been done

by introducing three different electron donating groups viz. -OC_2H_5, -SCH_3, -$N(CH_3)_2$ and two electron withdrawing grs viz. -CN, -NO_2 on the phenylene moiety of TPA unit of the dye systems. Hence a family of 18 TPA dye systems has been analyzed. Here, vinyl pyrrole is chosen as the extension of π-spacer. The advantage of the pyrrole moieties as the π-spacer is that it creates better charge separation in the excited states of the dye which arises from less interaction with its neighboring aromatic units.[42] Furthermore, vinylene groups offer a more flexible polymer chain, which could improve solubility compared to directly-coupled aryl-aryl conjugated polymers.[7] By increasing the π-conjugation of the linker, the HOMO and LUMO energy levels can be tuned. Benzothiadiazole-based dyes show a wide coverage of the solar spectrum.[8] Such a broad absorption is greatly beneficial to the improvement of photocurrent density and power-conversion efficiency of the dyes. Here we used three different benzothiadiazole derivatives as a π-spacer to construct all the dye systems. So by incorporating both electron-rich and electron-deficient moieties into TPA unit our aim is to understand how photovoltaic parameters are tuned on substitution, as well as to find out the optimum dye system within the selected dyes.

MODEL AND COMPUTATION

All the calculations have been performed by using the Gaussian 03W[43] program suite. The geometries of the dyes in gas phase were optimized using density functional theory (DFT)[44] with the B3LYP[45] hybrid functional and the 6-311G* basis set. The use of B3LYP/6-311G* or B3LYP/6-31G* level of theory for computing the geometry and electronic structure of TPA-based dyes are well tested and reported in the literature.[17,46] Furthermore, to calibrate our level of theory, we performed some test calculations on some TPA-based dyes whose experimental orbital energies are already reported. We observe a reasonable good comparison between the calculated and experimentally observed results. As for example, from differential pulse voltametry measurement and absorption spectra, the HOMO, LUMO energy for the dye TA-DM-CA were estimated to be -5.51

and -3.02 eV,[47] respectively, while our B3LYP/6-311G* calculation gives the same values at -5.23 and -2.73 eV, respectively. The more deviation in estimating LUMO energy is well assigned in DFT due to weak correlation effect. All the optimized geometries were subjected to vibrational analysis and characterized as at energy minimum (no imaginary frequency). The time-dependent DFT (TD-DFT) calculations were carried out to determine at least 30 vertical excitations to the excited state of the molecules. We wish to remember that TD-DFT at B3LYP has known problems of self-interaction errors particularly for D/A systems as charge transfer interactions are poorly accounted here.[48] Although more time consuming, the use of range separated DFT functionals is good way to treat this problem. Based on the optimized molecular structures of the dyes we simulated the UV-vis spectra of all of them in gas phase as well as solvent phase (methanol) with PBE1PBE hybrid function using same basis functions. The DFT functional PBE1PBE contains no empirical parameters and reported to reproduce good electronic properties in gas phase as well as solvent phase within reasonable computational resources.[49] In solvent phase (methanol), the computations were performed by applying polarisable continuum model (PCM) using the integral equation formalism variant (IEFPCM) to describe the electrostatic solute solvent interactions by the creation of solute cavity via a set of overlapping spheres.[50] The absorption spectra were simulated by using the 30 lowest spin-allowed singlet transitions, and finally the spectral data were plotted using mixed Lorentziane Gaussian lineshape (0.5) and an average full-width at the half maximum (3000 cm^{-1}) for all peaks.

RESULTS AND DISCUSSION

Geometry and electronic structure of the dyes:

As we have already mentioned in the previous section, we choose here mainly three types of dyes which are originated from triphenylamine (TPA) as the donor portion. Subsequent addition of different acceptors, namely thiadiazolothienopyazine, benzobis(thiadiazole), and benzothiadiazole group differs the dyes which are named as TPA-TBT-1, TPA-DBT-1, TPA-BT-1, respectively. The

optimized geometries of the dyes are shown shown in Fig. 1. To anchor the proposed dyes onto the semiconductor surface, however, an anchoring group, namely cyanoacrylic acid, has been attached to each of the dyes at the acceptor portion. Table 1 shows some of the geometric parameters, especially some selected dihedral angles. It is expected that an efficient dye should maintain the co-planarity between the anchoring group and the bridging unit so as to facilitate the electron transfer process from the donor moiety to the semiconductor surface. It is revealed from Table 1 that the dyes TPA-DBT-1 and TPA-BT-1 are more coplanar than TPA-TBT-1 indicating better electron delocalization and hence susceptible to better intramolecular charge transfer. Coplanerity, on the other hand, facilitates the recombination process also, which in turns decreases the efficiency of the dye as photovoltaic material. So, it requires a balance between charge transfer and electron recombination process.

To get further insight into the molecular structure and electronic distribution of these dyes, we have performed a molecular orbital analysis (MOA). In this regard, few occupied and unoccupied molecular orbitals are of particular interest, since they might be involved in the electron transfer process. However, upon photoexcitation, one electron of the HOMO of the dye is transferred to the LUMO which thereafter participate in the subsequent energy injection processes. Fig. 2 depicts the electron density distribution of the some frontier molecular orbitals of the dyes. It is clear from the figure that the HOMOs of the dyes are more concentrated over the donor part (TPA moiety) and its adjacent π-spacer (vinyl pyrrole group) while the LUMOs are more concentrated over the acceptor and the adjacent cyanoacrylic acid (anchoring) group. The situation becomes more prominent when some electron withdrawing groups are attached to the donor moiety which has been discussed later. Thus a spatial separation of the electron density within the dye molecule indicates facilitation of the electron transfer processes from dye to semiconductor surface through photoexcitation which is one of the crucial point to be an efficient dye useful for DSSC. It is evident that for the dyes TPA-TBT-1 and TPA-BT-1 this spatial separation is more prominent and consequently these are expected to perform in a better way. The HOMO-LUMO gaps (Δ) of the dyes are depicted in Table 2 which shows that TPA-TBT-1 and TPA-DBT-1 dyes have Δ

values in the order of 1.3 eV, whereas the same for the dye TPA-BT-1 is much higher and in the order of 1.60 eV. However, as also indicated from the energy positions of the HOMO and LUMO of the dyes, we expect to have type-II band alignment in most of the cases while attaching the dyes with TiO_2 semiconducting surface, keeping in the mind that, in the composite system, the quasiparticle energy levels are tunable depending upon the nature of dye-adsorbent interaction.[51] It is noteworthy to mention here that use of TiO_2 semiconducting surface as a sink of photoelectron in solar cell is well tested and is of crucial interest in recent days and we use TiO_2 surface referring the value of E_{CB} = 4.0 eV as reported by Asbery et al.[15] Note that, the band bending as evident from the recent studies[51,52] may alter the conduction abnd edge of TiO_2 surface which has a direct infuence on the performance of a DSSC, although a very recent expriment demonstrates the higher photocatalytic activity of anatase surface of TiO_2 under flat-band condition[53]

Effects of chemical modifications:

The electron injection process and hence efficiency of a dye in DSSC is governed by the relative position of the energy levels of the dye with respect to the CBM of the semiconductor surface. Interestingly, the most prominent feature of the organic dye is the tunability of these energy levels by introducing various functional groups especially to the donor moiety. For this purpose, we choose three electron donating groups namely, -OC_2H_5, -SCH_3, -$N(CH_3)_2$ and two electron withdrawing groups -NO_2, -CN. The unsubstituted and the substituted dyes are named with suffixes 1-6, respectively. It is worthy to mention here that all the groups are introduced at the donor part, firstly because the introduction of electron donating groups at the π-spacer increases steric repulsion and secondly the electron withdrawing group at the π-spacer induces a negative effect on the DSSCs efficiency as reported by Sun and co-workers.[54] This is because the electron-withdrawing units on the π-spacer suppress the electron injection from the LUMO level to the semiconductor conduction band. It is also to be noted that functionalizing the acceptor part here creates a sever steric hindrance retarding the charge transfer process. Table 2 depicts how the electronic energy levels of the dyes are changed upon substitution of different functional groups. The HOMO and

LUMO energy levels of the dyes TPA-TBT-1, TPA-DBT-1, and TPA-BT-1 are -5.02, -5.23, -5.32 eV and -3.68, -3.92, -3.72 eV, respectively. These values indicates that HOMO energy in dye TPA-BT-1 is significantly lowered due to the presence of benzothiadiazole group. In TPA-DBT-1 the LUMO level is greatly stabilized due to the highly electron withdrawing benzobis(thiadiazole) group which is reflected by the low band gap 1.30 eV of TPA-DBT-1. Now, concerning the effect of substituents on the donor moiety of the dye it is revealed that, attaching -CN and $-NO_2$ groups on the phenyl ring of triphenylamine, it stabilizes both the HOMOs and LUMOs of TPA-TBT-5, and TPA-TBT-6. The substituent $-N(CH_3)_2$ offers very low band gap in TPA-TBT-4 (1.10 eV) but for which the HOMO energy level is situated slightly higher than the reduction potential energy of the I_3^-/I^- electrolyte (-4.80 eV). The $-OC_2H_5$ group destabilises the HOMO energy and reduces the band gap to 1.26 in the dye TPA-TBT-2. Among the substituted structures of TPA-DBT-1 the dye TPA-DBT-4 is quite interesting for which the presence of $-N(CH_3)_2$ group stabilizes both the HOMO and LUMO, and a very low and gap (1.145 eV) is achieved. $-OC_2H_5$ group in TPA-DBT-2 offers a band gap of 1.25 eV. In the substituted forms of TPA-BT-1 dyes the band gap of TPA-BT-4 is lowest 1.45 eV due to the strong electron donating effect of $-N(CH_3)_2$ group. The HOMO and LUMO energy levels of all the TPA-BT dyes (TPA-BT-1-6) full fill the requirements of a good sensitizer.

Electron transfer and photovoltaic activities:

As already mentioned, suitable energy band alignment is necessary to acquire a desired photovoltaic performance. Thermodynamically, for the spontaneous charge transfer process from the excited state of the dye to conduction band of TiO_2 requires LUMO energy of the dye to be at more positive potential than conduction band of TiO_2 (-4.0 eV) while HOMO energy of the dye should be more negative than reduction potential energy of the I_3^-/I^- electrolyte (-4.80 eV). As displayed in Table 2, chemical substitution to the dye molecule changes the relative position of the frontier energy levels in an substantial amount which affects the charge transfer process. As for example, dimethylammine ($-N(CH_3)_2$) rises up the LUMO level of the TPA-TBT-1 by an amount of

0.09 eV thereby increasing the electron injection rate from photo-excited dye to the TiO_2 surface. According to Marcus theory of electron injection which states that, the larger the value of ΔG_{inject}, the faster the rate of electron injection. It is worthy to mention here that this assumption is valid as long as the injection is restricted to energy levels close to the conduction band edge and that the density of the acceptor states in this energy range remains constant.[55] It is clear from Table 2 that the LUMOs of all dyes (except TPA-DBT-3, TPA-DBT-5, TPA-DBT-6) lie over the E_{CB} of TiO_2 and the HOMOs are situated below the redox potential of I_3^-/I^- electrolyte (-4.80 eV). Thus, it can be stated that all of them (except TPA-DBT-3,5,6) possesses a positive response to charge transfer and regeneration related to photooxidation process. Fig. 3 displays the relative energy levels of some selective dyes with reference to conduction band of TiO_2 surface and triiodide/iodide as the redox couple. The figure depicts that TPA-BT-2 is expected to show the fastest electron transfer among the dyes studied here. Our prediction is also supported by greater charge separation in the HOMO and LUMO of this specified dye as could be found in Fig. 4.

Absorption properties:

Based on the optimized molecular structures with B3LYP/6-311G* method we calculated the UV-vis spectra of the dyes using TD-DFT calculations in methanol with PEB1PBE hybrid functional taking the lowest 30 spin-allowed singlet-singlet transitions into account. Before computing the UV-vis spectra the dipole moment values of the individual dye systems have been analyzed and are tabulated in the Table 3. The high dipole moment values indicate that all the dyes are polar. Table 3 also provides the vertical excitation energy (E*), oscillator strength (f), and also the light harvesting capacities (LHC) of the parent and the substituted dyes.

All the dyes shows a broad UV-Vis spectra whose tails enter into the IR region rendering a broad light harvesting power. In Fig. 5 we have shown the computed UV-Vis. spectra of some representative dyes in methanol solvent. It is clear from the figure that all the dyes show two absorption peaks, one in visible region (around 500 nm) and other in the far infrared region; the corresponding values of maximum absorption wavelength (λ_{max}) for all the dyes are given in Table

3. For the dye TPA-TBT-1, the λ_{max}=543 nm is assigned to be mainly due to HOMO→LUMO+2 transition, whereas the second broad absorption peak at 1566 nm corresponds to HOMO-LUMO transition. On the other hand, for other two dyes the HOMO-LUMO transition becomes the highest intensity peak which can be interpreted by the more co-planer nature of TPA-DBT-1 and TPA-BT-1 than that of TPA-TBT-1. Table 3 also indicates that there is pronounced effect on the λ_{max}, and oscillator strength and hence LHC with substitution. For most of the substituted dye systems there is a increased oscillator strength than the corresponding main dye system which may be ascribed as the better π-conjugation. We have also calculated the LHC which is another factor which determines the efficiency of DSSC. Highest oscillator strength and hence high LHC is found for TPA-DBT-2. λ_{max} is found to be the highest for TPA-TBT-4 dye for which LHC is 0.8324. From the calculated data it can also be inferred that in case of electron donating -OC_2H_5 substituent there is always a higher value of λ_{max}, oscillator strength and LHC as compared to the corresponding unsubstituted dye.

The overall efficiency (η) of the DSSC can be computed from the short-circuit photocurrent density (J_{SC}), open cir-cuit potential (V_{OC}), the fill factor (FF) and the intensity of incident solar light (P_{inc}) as expressed in equation (1). The values of J_{SC}, V_{OC}, and FF can be obtained from the current-voltage characteristics in the illuminated condition and are beyond our scope. Only analytical relationship between V_{OC} and E_{LUMO} of the dye may be expressed as: $eV_{OC}=E_{LUMO}-E_{CB}$, where (E_{CB}) is the conduction band energy of the semiconductor surface. It induces that the higher the value of E_{LUMO}, larger is that for V_{OC}. The computed values of eV_{OC} for the dyes are given in Table 3 which depicts that V_{OC} is maximum for TPA-BT-4.

CONCLUSION

In the present work, we managed to bring out different structural modifications that will optimize the photovoltaic properties of the TPA-based DSSCs. We use this theoretical procedure to gain insights into the geometrical and electronic structures of the dyes. All the dyes except TPA-DBT-3,

TPA-DBT-5, and TPA-DBT-6 are found to fulfill the criteria for using in an efficient dye sensitized solar cell. The substituents are found to have huge effect on the optoelectronic properties of the dyes. Substitution of -OC_2H_5 group emerged to be most successful. In all the dyes -OC_2H_5 substitution resulted in increase of open circuit voltage, significant decrease in band gap and remarkable increase in oscillator strength. So, it can be concluded that substitution of -OC_2H_5 group is suitable to meet the needs of efficient dye. While substitution of -$S(CH_3)_3$ group hasn't been much successful. Only in case of TPA-BT it lowers the band gap, and in every case it has lowered the oscillator strength and open circuit voltage value. Substitution of -$N(CH_3)_3$ resulted all along positively in case of TPA-TBT leading to a decrease in band gap, increase in oscillator strength and consequently LHE, and a significant increase in open circuit voltage. While in case of other two dyes it gives mixed results. In both cases it lowers the band gap and increases the open circuit voltage but decreases the oscillator strength. -NO_2 substitution is also not very successful. Other than TPA-BT it increases the band gap and in every cases it has lowered the open circuit voltage. Oscillator strength has increased in TPA-TBT but not in the other two cases. -CN substitution shows almost the similar results. We strongly believe that our theoretical stydy will be stimulus for the experimentalists and the guideline provided by these studies will be verry effective for experimental design and fabrication of the TPA-based photovoltaic devices.

ACKNOWLEDGMENT

The authors sincerely acknowledge UGC, New Delhi, Govt. of India for partial financial support. The financial support from SERB-DST, New Delhi through the project Ref. No. CS-085/2014 is gratefully acknowledged. PS acknowledges the financial support from CSIR [01(2744)/13/EMR-II]. AP gratefully acknowledges Dr. D.S. Kothari Postdoctoral Fellowship provided by UGC, New Delhi.

References

(1) B. ÓReagan and M. Grätzel, *Nature*, 1991, **353**, 73

(2) M. Grätzel, *Nature*, 2001, **414**, 338.

(3) M. K. Nazeeruddin, F. D. Angelis, S. Fantacci, A. Selloni, G. Viscardi, P. Liska, S. Ito, B. Takeru and M. Grätzel, *J. Am. Chem. Soc.*, 2005, **127**, 16835.

(4) C.-Y. Chen, M. K. Wang, J.-Y. Li, N. Pootrakulchote, L. Alibabaei, C. H. Ngoc-le, J. D. Decoppet, J .H. Tsai, C. Grätzel, C. G. Wu, et al. *ACS Nano*, 2009, **3**, 3103.

(5) Y. Saito, N. Fukuri, R. Senadeera, T. Kitamura, Y. Wada and S. Yanagida, *Electrochem. Commun.*, 2004, **6**, 71.

(6) J. B. Asbury, R. J. Ellingson, H. N. Ghosh, S. Ferrere, A. J. Nozik and T. Lian, *J. Phys. Chem. B*, 1999, **103**, 3110.

(7) J. H. Werner, Second and Third Generation Photovoltaics-Dreams and Reality. In Advances in Solid State Physics; B. Kramer, Ed.; Springer: Berlin Heidelberg, Germany, 2004; **Volume 44**, pp. 172-172.

(8) R. Argazzi, G. Larramona, C. Contado and C. A. Bignozzi, *J. Photochem. Photobiol. A Chem.*, 2004, **164**, 15-21.

(9) Y. Koyama, T. Miki, X.-F. Wang and H. Nagae, *Int. J. Mol. Sci.*, 2009, **10**, 4575.

(10) T. Kitamura, M. Ikeda, K. Shigaki, T. Inoue, N. A. Anderson, X. Ai, T. Q. Lian and S. Yanagida, *Chem. Mater.*, 2004, **16**, 1806.

(11) G. Yu, J. Gao, J. C. Hummelen, F. Wudl and A. Heeger, *J. Science*, 1995, **270**, 1789.

(12) Y. J. Cheng, S. H. Yang and C. S. Hsu, *Chem. Rev.*, 2009, **109**, 5868.

(13) T.-Y. Chu, J. Lu, S. Beaupré, Y. Zhang, J.-R. Pouliot, S. Wakim, J. Zhou, M. Leclerc, Z. Li, J. Ding and Y. Tao, *J. Am. Chem. Soc.*, 2011, **133**, 4250.

(14) D. Cahen, G. Hodes, M. Gräetzel, J. F. Guillermoles and I. J. Riess, *J. Phys. Chem. B*, 2000, **104**, 2053.

(15) J. B. Asbury, Y. Q. Wang, E. Hao, H. N. Ghosh and T. Lian, *Res. Chem. Intermed.*, 2001, **27**, 393.

(16) W. Sang-aroon, S. Saekow and V. Amornkitbamrung, *J. Photochem. Photobiol. A: Chem.*, 2012, **236**, 35.

(17) J. Preat, C. Michaux, D. Jacquemin and E. A. Perpète, *J. Phys. Chem. C*, 2009, **113**, 16821.

(18) C. J. Brabec, C. Winder, N. S. Sariciftci, J. C. Hummelen, A. Dhanabalan, P. A. van Hal and R. A. Janssen, *J. Adv. Funct. Mater.*, 2002, **12**, 709.

(19) J. J. M. Halls, J. Cornil, D. A. dos Santos, R. Silbey, D.-H. Hwang, A. B. Holmes, J. L. Brdas and R. H. Friend, *Phys. Rev. B.*, 1999, **60**, 5721.

(20) A. Hagfeldt, G. Boschloo, L. Sun, L. Kloo and H. Pettersson, *Chem. Rev.*, 2010, **110**, 6595.

(21) A. Mishra, M. K. R. Fischer and P. Buerle, *Angew. Chem. Int. Ed.*, 2009, **48**, 2474.

(22) R. Kroon, M. Lenes, J. C. Hummelene, P. W. M. Blom and B. De Boe, *Polymer Reviews*, 2008, **48**, 531.

(23) Handbook of Organic Conductive Molecules and Polymers, H. S. Nalwa, *John Wiley and Sons*, 1999.

(24) E. Lim, B.-J. Jung, H.-K. Shim, T. Taguchi, B. Noda, T. Kambayashi, T. Mori, K. Ishikawa, H. Takezoe and L.-M. Do, *Org. Electron.*, 2006, **7**, 121.

(25) Z. Ning and H. Tian, *Chem. Comm.*, 2009, 5483.

(26) Z. Ning, Q. Zhang, W. Wu and H. Tian, *J. Org. Chem.*, 2008, **733**, 3791.

(27) D. Liu, R. W. Fessenden, G. L. Hug and P. V. Kamat, *J. Phys. Chem. B*, 1997, **101**, 2582.

(28) S. Erten-Ela, M. Marszalek, S. Tekoglu, M. Can and S. Icli, *Curr. Appl. Phys.*, 2010, **10**, 749.

(29) M. Liang, W. Xu, F. S. Cai, P. Q. Chen, B. Peng, J. Chen and Z. M. Li, *J. Phys. Chem. C*, 2007, **111**, 4465.

(30) J. Tang, W. Wu, J. Huan, J. Li, X. Li and H. Tian, *Energy Environ. Sci.*, 2009, **2**, 982.

(31) J. Shi, J. Huang, R. Tang, Z. Chai, J. Hua, J. Qin, Q. Li and Z. Li, *Eur. J. Org. Chem.*, 2012, 5248.

(32) S. P. Singh, M. S. Roy, K. R. J. Thomas, S. Balaiah, K. Bhanuprakash and G. D. Sharma, *J. Phys. Chem. C*, 2012, **116**, 5941.

(33) J. H. Yum, D. P. Hagberg, S. J. Moon, K. M. Karlsson, T. Marinado, L. C. Sun, A. Hagfeldt, M. K. Nazeeruddin and M. Grätzel, *Angew. Chem. Int. Ed.*, 2007, **48**, 1576.

(34) L. Alibabaei, J. H. Kim, M. Wang, N. Pootrakulchote, J. Teuscher, D. Di Censo, R. Humphry-Baker, J. E. Moser, Y. J. Yu, K. Y. Kay, S. M. Zakeeruddin and M. Grätzel, *Energy Environ. Sci.*, 2010, **3**, 1757.

(35) Y. S. Yen, Y. C. Hsu, J. T. Lin, C. W. Chang, C. P. Hsu and D. J. Yin, *J. Phys. Chem. C*, 2008, **112**, 12557.

(36) Q. Q. Li, J. Shi, H. Y. Li, S. Li, C. Zhong, F. L. Guo, M. Peng, J. L. Hua, J. G. Qina and Z. Li, *J. Mater. Chem.*, 2012, **22**, 6689.

(37) W. Zeng, Y. Cao, Y. Bai, Y. Wang, Y. Shi, M. Zhang, F. Wang, C. Pan and P. Wang, *Chem. Mater.*, 2010, **22**, 1915.

(38) A. Dualeh, F. De Angelis, S. Fantacci, T. Moehl, C. Y. Yi, F. Kessler, E. Baranoff, M. K. Nazeeruddin and M. Grätzel, *J. Phys. Chem. C*, 2012, **116**, 1572.

(39) J. X. He, F. L. Guo, X. Li, W. J. Wu, J. B. Yang and J. L. Hua, *Chem. Eur. J.*, 2012, **18**, 7903.

(40) M. Mba, M. ĎAcunzo, P. Salice, T. Carofiglio, M. Maggini, S. Caramori, A. Campana, A. Aliprandi, R. Argazzi, S. Carli, et al. *J. Phys. Chem. C*, 2013, **117**, 19885.

(41) G. Wu, F. Kong, Y. Zhang, X. Zhang, J. Li, W. Chen, W. Liu, Y. Ding, C. Zhang, B. Zhang, J. Yao and S. Dai, *J. Phys. Chem. C*, 2014, **118**, 8756.

(42) K. R. J. Thomas, J. T. Lin, Y. C. Hsu and K. C. Ho, *Chem. Commun.*, 2005, 4098.

(43) M. J. Frisch, G. W. Trucks, H. B. Schlegel, G. E. Scuseria, M. A. Robb, J. R. Cheeseman, G. Scalmani, V. Barone, B. Mennucci, G. A. Petersson, et al. *Gaussian 03*, revision C.02; Gaussian, Inc.: Wallingford, CT, 2004.

(44) R. Ditchfield, W. J. Herhe and J. A. Pople, *J. Chem. Phys.*, 1971, **54**, 724.

(45) A. D. Beche, *J. Chem. Phys.*, 1993, **98**, 5648.

(46) S. Haid, M. Marszalek, A. Mishra, M. Wielopolski,J. Teuscher, J.-E. Moser, R. Humphry-Baker, S. M. Zakeeruddin, M. Grätzel, and P. Bäuerle, *Adv. Funct. Mater.*, 2012, **22**, 1291.

(47) H. Im, S. Kim, C. Park, S.-H. Jang, C.-J. Kim, K. Kim, N.-G. Park and C. Kim, *Chem. Commun.*, 2010, **46**, 1335.

(48) C. Sutton, T. Körzdörfer, V. Coropceanu and J.-L. Brédas, *J. Phys. Chem. C*, 2014, **118**, 3925.

(49) M. D. Liptak and G. C. Shields, *Int. J. Quant. Chem.*, 2005, **105**, 580.

(50) S. Miertus and J. Tomasi, *Chem. Phys.*, 1982, **65**, 239.

(51) S. Md. Pratik and A. Datta, *Phys. Chem. Chem. Phys.*, 2013, **15**, 18471.

(52) J. Feng, Y. Jiao, W. Ma, Md. K. Nazeeruddin, M. Grätzel and S. Meng, *J. Phys. Chem. C*, 2013, **117**, 3772.

(53) K. Ozawa, M. Emori, S. Yamamoto, R. Yukawa, S. Yamamoto, R. Hobara, K. Fujikawa, H. Sakama and I. Matsuda, *J. Phys. Chem. Lett.*, 2014, **5**, 1953.

(54) R. Chen, X. Yang, H. Tian and L. Sun, *J. Photochem. Photobiol. A. Chem.*, 2007, **189**, 295.

(55) R. A. Marcus and N. Sutin, *Biochem. Biophys. Acta*, 1985, **811**, 265.

Table 1: Some specific dihedral angles of the optimized dyes.

Name of the Dye	Dihedral angle (Degree)	
	C1-C2-C3-C4	C5-C6-C7-C8
TPA-TBT-1	29.55	-28.36
TPA-DBT-1	1.17	-30.06
TPA-BT-1	0.19	-0.05

Table 2: Frontier molecular orbital energy levels (with respect to vacuum) and the corresponding optical gap of the different dyes.

Dye	E_{HOMO} (eV)	E_{LUMO} (eV)	Δ (eV)
TPA-TBT-1	-5.02	-3.68	1.35
TPA-TBT-2	-4.84	-3.59	1.26
TPA-TBT-3	-5.05	-3.70	1.35
TPA-TBT-4	-4.61	-3.51	1.10
TPA-TBT-5	-5.46	-3.93	1.53
TPA-TBT-6	-5.41	-3.91	1.51
TPA-DBT-1	-5.23	-3.92	1.30
TPA-DBT-2	-5.05	-3.80	1.25
TPA-DBT-3	-5.34	-4.01	1.34
TPA-DBT-4	-4.83	-3.68	1.15
TPA-DBT-5	-5.71	-4.28	1.43
TPA-DBT-6	-5.65	-4.23	1.41
TPA-BT-1	-5.32	-3.72	1.60
TPA-BT-2	-5.13	-3.62	1.51
TPA-BT-3	-5.46	-3.80	1.66
TPA-BT-4	-4.74	-3.25	1.49
TPA-BT-5	-5.81	-3.79	2.02
TPA-BT-6	-5.74	-3.75	1.99

Table 3: Vertical excitation energy, dipole moment, and some photovoltaic parameters of the dyes.

Dye	E* (eV)	λ_{max} (nm)	f	LHC	(eV_{OC})	μ
TPA-TBT-1	2.28	543	0.611	0.75	0.32	8.1
TPA-TBT-2	0.76	1640	0.643	0.77	0.41	12.3
TPA-TBT-3	2.25	551	0.615	0.76	0.30	9.8
TPA-TBT-4	0.67	1841	0.776	0.83	0.49	14.5
TPA-TBT-5	2.48	499	0.632	0.77	0.06	5.1
TPA-TBT-6	2.37	523	0.850	0.86	0.09	4.6
TPA-DBT-1	1.05	1185	0.956	0.89	0.08	17.7
TPA-DBT-2	0.99	1252	1.026	0.91	0.20	22.3
TPA-DBT-3	1.04	1193	0.898	0.87	- 0.01	16.2
TPA-DBT-4	0.86	1445	1.066	0.91	0.32	25.4
TPA-DBT-5	1.14	1089	0.768	0.83	-0.28	7.7
TPA-DBT-6	1.08	1153	0.742	0.82	-0.23	8.5
TPA-BT-1	1.10	1126	0.826	0.85	0.28	12.9
TPA-BT-2	1.02	1215	0.859	0.86	0.38	17.1
TPA-BT-3	1.11	1112	0.782	0.83	0.20	11.7
TPA-BT-4	0.86	1442	0.807	0.84	0.75	18.1
TPA-BT-5	1.40	886	0.766	0.83	0.21	0.7
TPA-BT-6	1.29	962	0.649	0.78	0.25	1.6

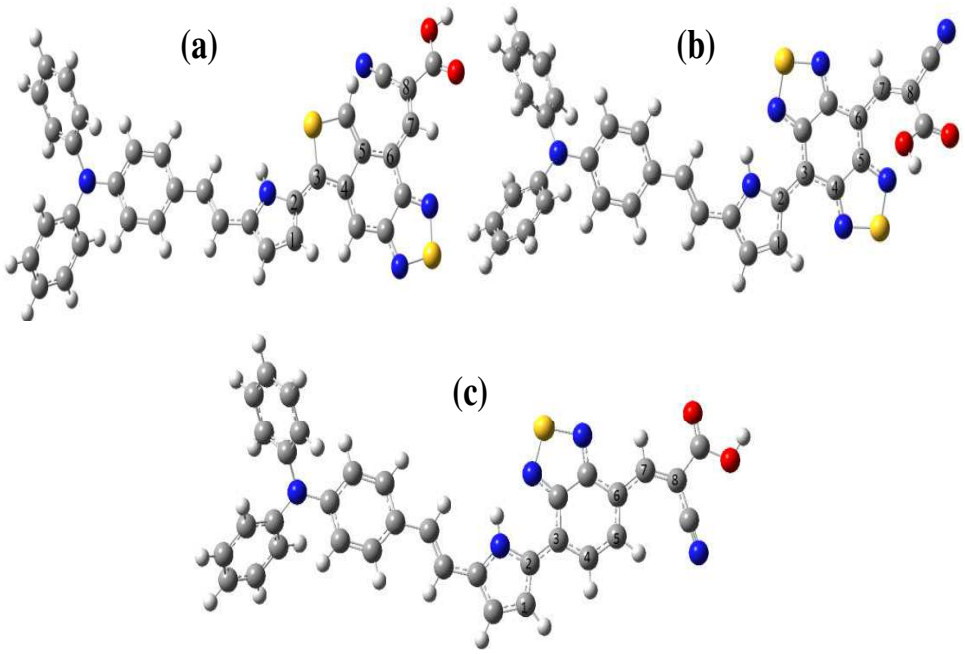

Figure 1: Optimized ground state geometries of the dyes (a) TPA-TBT-1, (b) TPA-DBT-1, (C) TPA-BT-1 in gas phase obtained at the B3LYP/6-311G(d,p) level of theory.

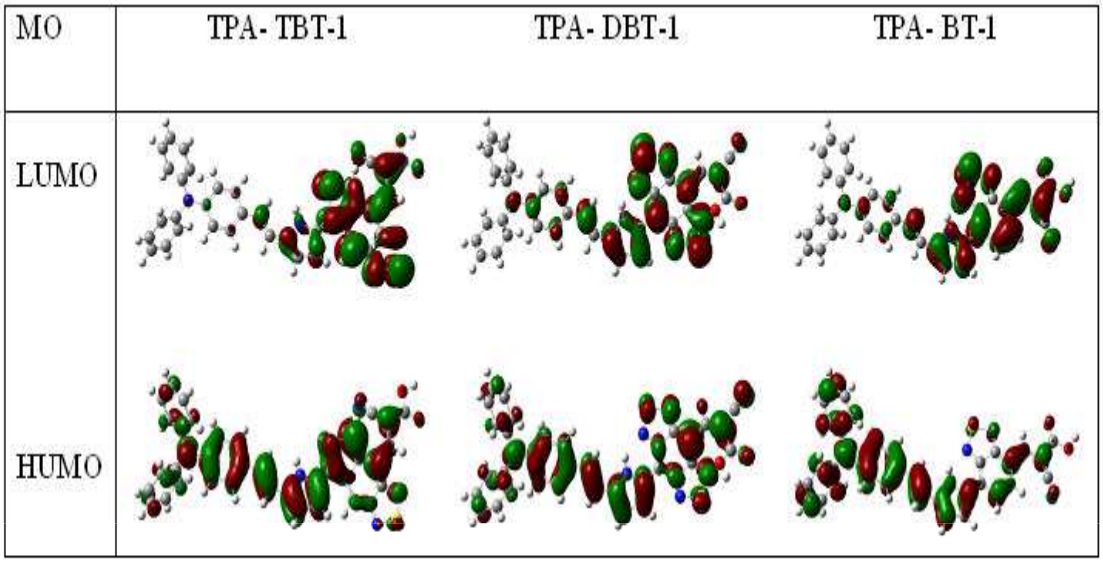

Figure 2: Representation of HOMO, and LUMO diagram of TPA-TBT-1, TPA-DBT-1 and TPA-BT-1.

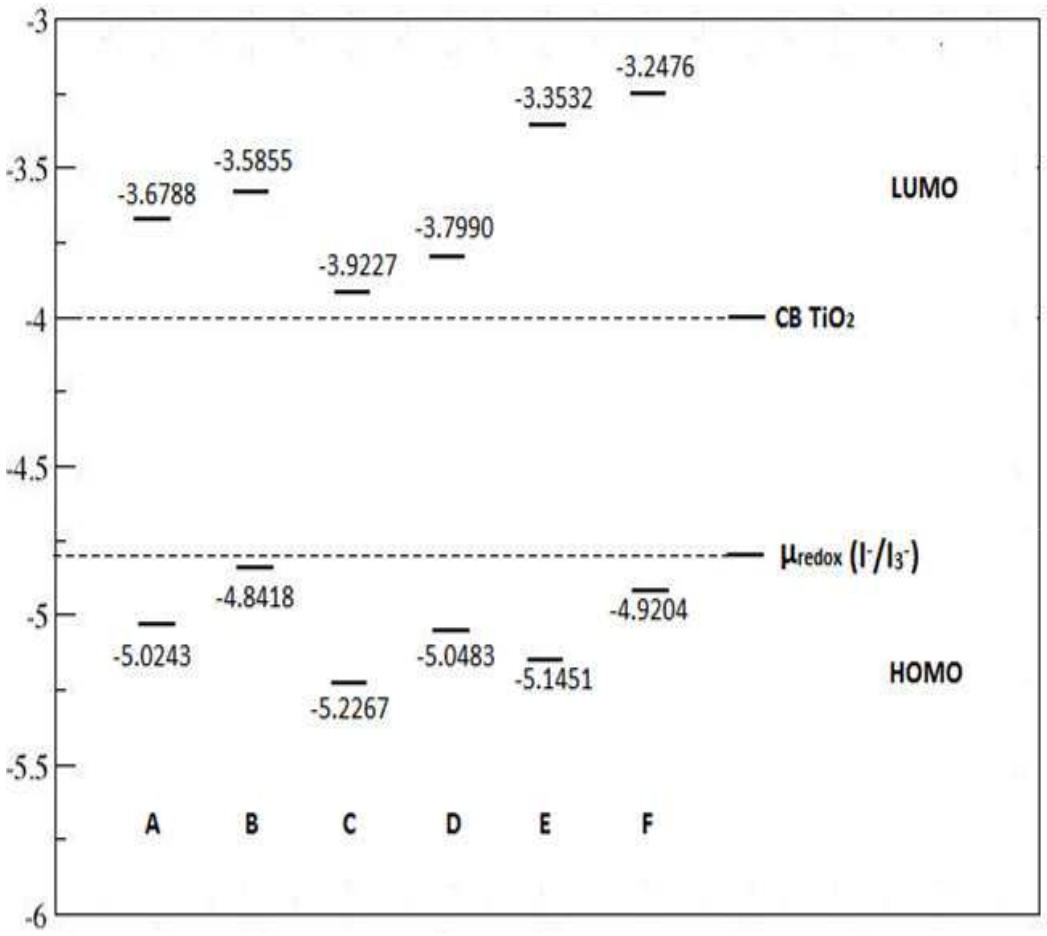

Figure 3: HOMO and LUMO energy level diagram of (A) TPA-TBT-1 (B) TPA-TBT-2 (C) TPA-DBT-1 (D) TPA-DBT-2 (E) TPA-BT-1 (F) TPA-BT-2.

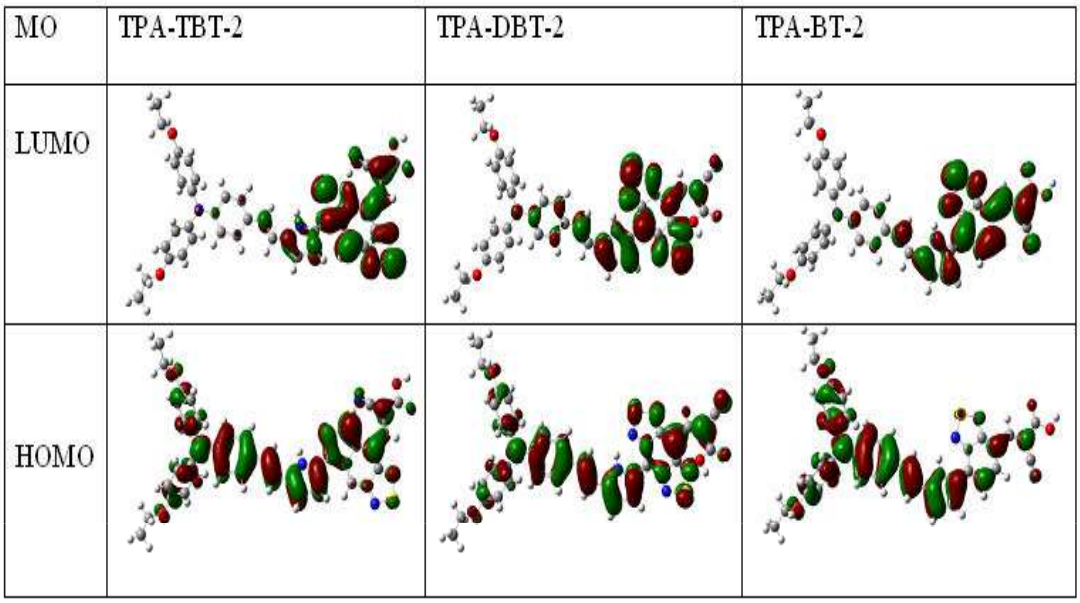

Figure 4: HOMO, and LUMO diagram of TPA-TBT-2, TPA-DBT-2, and TPA-BT-2. They have been obtained at the B3LYP/6-311G(d,p) level.

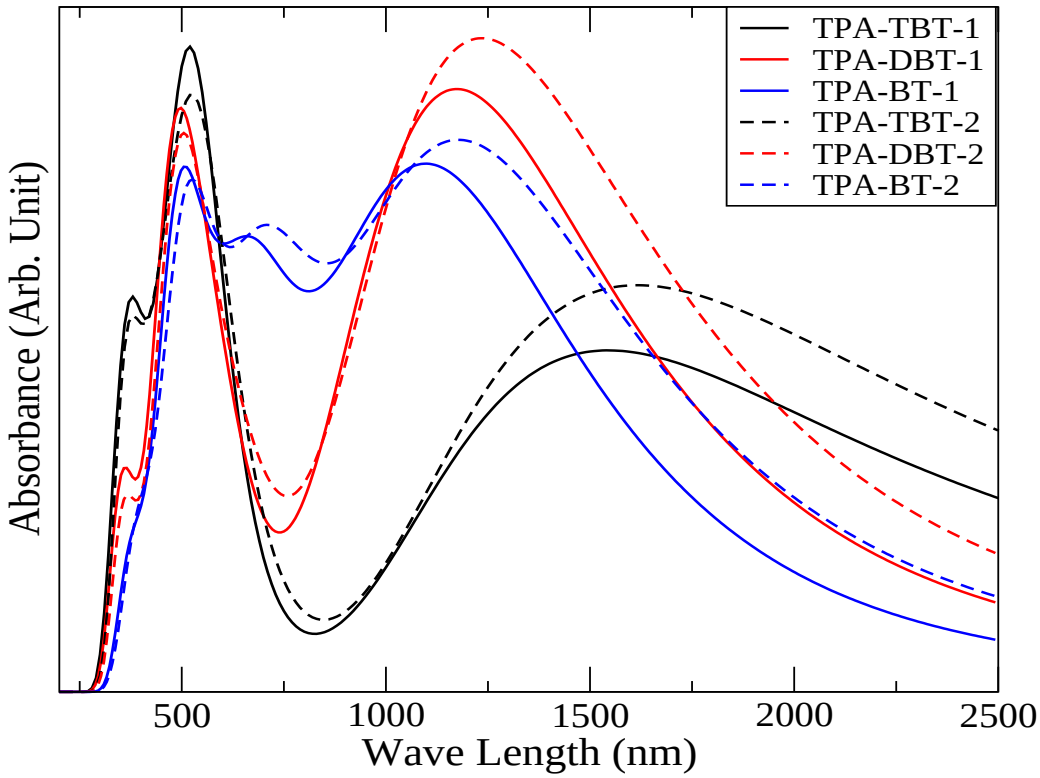

Figure 5: Simulated UV-Vis. absorption spectra of some selected dyes.